

# Spectroscopic study of optically induced ultrafast electron dynamics in gold

V. V. Kruglyak\* and R. J. Hicken

*School of Physics, University of Exeter, Stocker Road, Exeter EX4 4QL, United Kingdom*

P. Matousek and M. Towrie

*Central Laser Facility, CCLRC Rutherford Appleton Laboratory, Chilton, Didcot, Oxfordshire OX11 0QX, United Kingdom*

(Received 24 March 2006; revised manuscript received 13 July 2006; published 12 January 2007)

Using a supercontinuum pulse as a probe, we have measured the transient reflectivity spectra of a thin film of gold for different values of the pump-probe time delay. The wavelength  $\lambda_x$  at which the measured transient reflectivity changes sign has been found to depend upon the time delay, leading to bipolar time resolved signals. The time dependence of  $\lambda_x$  has been shown to be consistent with calculations that take into account the full dependence of the reflectivity upon the electron occupation number, and to contradict qualitatively a model in which the signal is assumed to be directly proportional to the occupation number. The shift of  $\lambda_x$  has been found to persist at time delays that are much longer than the time required for the electrons to thermalize. Therefore the bipolar reflectivity signals do not necessarily contain a contribution from nonthermalized electrons, as has been previously assumed.

DOI: [10.1103/PhysRevB.75.035410](https://doi.org/10.1103/PhysRevB.75.035410)

PACS number(s): 78.47.+p, 78.66.Bz, 78.20.Bh

## I. INTRODUCTION

Optical pump-probe measurements using femtosecond lasers have proven to be a very sensitive tool for the investigation of electron and spin dynamics in solids. They have been used to study many phenomena of fundamental and applied interest such as optical orientation of spin,<sup>1</sup> ultrafast demagnetization,<sup>2</sup> and ultrafast excitation of coherent phonons,<sup>3</sup> and magnons.<sup>4</sup> Their potential for materials characterization is illustrated by measurements of the electron-phonon coupling constant in high  $T_c$  superconductors<sup>5</sup> and metals,<sup>6</sup> hot electron linear and angular momentum relaxation times<sup>7</sup> and nonlinear susceptibility tensor components<sup>8</sup> in metals, and the spin wave mode spectrum of nanomagnets.<sup>9</sup>

Significant efforts have been devoted recently to investigations of the kinetics of electron-electron and electron-phonon thermalization in metals, deduced from measurements of the transient (differential) reflectivity and/or transmission. Often, the transient signal is analyzed by assuming that it depends linearly upon either the transient electron (and lattice) temperature,<sup>6,10</sup> or the transient excess total electron energy,<sup>11</sup> or the transient electron occupation number.<sup>12</sup> However, such an assumption (referred to as the “linearity assumption” from hereon) is not self-consistent since transient reflectivity and transmission signals appear to have a different temporal shape,<sup>13–18</sup> and hence cannot be both proportional to the same function of time, e.g., the transient electron temperature. As has been known since the early optical thermomodulation studies of metals,<sup>19</sup> rigorous analysis instead requires the transient reflectivity and transmission to be properly calculated from the dependence of the complex dielectric function upon the electron occupation number. In practice, the full calculation was normally used only for simulation, while simplified analytical “response functions” were used to fit the data, thus implicitly making the *unjustified* assumption of linearity (see for example Refs. 13, 16, and 18). Since the differential reflectivity and transmission in fact have a nonlinear dependence upon the probe

wavelength and the electron occupation number (or temperature), conclusions reached using the linearity assumption now appear unreliable.

In this paper, we report optical pump and supercontinuum-probe<sup>12,18,20–23</sup> measurements of the transient reflectivity response of a thin film of gold over a wide spectral range. In the wavelength domain, we observe that the point at which the transient reflectivity spectra cross zero shifts with the time delay at which they were acquired. We show that this shift is incompatible with the arguments of Schoenlein *et al.* that were based upon the linearity assumption.<sup>12</sup> Due to the presence of the shift, time resolved signals reconstructed from the spectra become bipolar at wavelengths near the zero crossing point. Sun *et al.* also observed signals of similar bipolar shape, and interpreted them in terms of a short lived contribution from nonthermalized electrons.<sup>13</sup> We show that the shift is observed even for time delays as long as 10 ps, by which time the electron population is generally believed to have thermalized, and so the hot electron contribution to the transient reflectivity response of metals may be less significant than concluded by Sun *et al.* To further illustrate that the simplified analyzes based upon the linearity assumption are not self-consistent, we fit our time resolved signals to a solution of the modified two temperature model and show that the values of the fit parameters, that are expected to characterize the electron population as a whole, appear to be wavelength dependent. This emphasizes once again that a proper description of the temperature dependence of the metallic reflectivity may be essential for a correct interpretation of the experiments.

Due to its well-known optical properties,<sup>19,24</sup> gold has been the metal most widely studied in optical pump-probe measurements. A correct understanding of its transient reflectivity provides a basis for the understanding and quantification of experiments on other metals. Hence the sample of choice for our study was a  $(28.10 \pm 0.03)$  nm thick gold film with  $(1.30 \pm 0.01)$  nm roughness, magnetron sputtered on to a Si wafer substrate. The film was chosen to be thin enough to

reduce the electron heat transport in the direction perpendicular to its surface, while thick enough to minimize the effect of the substrate upon the measured reflectivity. To ensure the latter, experiments were performed on gold films of greater thickness. These yielded very similar results and so this additional data has not been included within the present paper.

## II. THEORY

Generally, absorption of a pump pulse does not directly affect the lattice, but leads to the creation of a nonequilibrium population of hot electrons. The scattering among the hot electron population as well as from the phonons, defects, etc., results in the creation of the equilibrium electron distribution described by the Fermi-Dirac function

$$f_{\text{FD}}(\varepsilon, T_e) = \frac{1}{\exp\left(\frac{\varepsilon - \varepsilon_{\text{F}}(T_e)}{k_{\text{B}}T_e}\right) + 1}, \quad (1)$$

where  $\varepsilon$  is the electron energy,  $T_e$  is the electron temperature,  $\varepsilon_{\text{F}}$  is the Fermi energy, and  $k_{\text{B}}$  is the Boltzmann constant. At moderate temperatures, the Fermi energy varies with temperature as

$$\varepsilon_{\text{F}}(T_e) = \varepsilon_{\text{F}0} \left[ 1 - \frac{\pi^2}{12} \left( \frac{k_{\text{B}}T_e}{\varepsilon_{\text{F}0}} \right)^2 \right] \theta, \quad (2)$$

where  $\varepsilon_{\text{F}0}$  is the Fermi energy at absolute zero temperature.

When the electrons have thermalized, the electron temperature can still be higher than that of the lattice. The main postulate of the two temperature model<sup>25</sup> is that the lattice and electron populations are well characterized by their respective temperatures which equalize with rate proportional to the electron-phonon coupling constant. The modified two temperature model takes into account the process of electron thermalization by assuming that the electrons may be divided into two subsystems one of which is in local thermal equilibrium while the other is not. The details of the nonequilibrium state are neglected, and both subsystems are characterized by the amount of excess energy that they possess relative to the unperturbed state. The excess energy of the thermalized electron subsystem is equal to the product of the excess electron temperature  $\Delta T_e$  and the electron heat capacitance  $C_e$ , which is in turn proportional to the electron temperature  $T_e = T_0 + \Delta T_e$ , where  $T_0$  is the ambient (unperturbed) temperature. The time dependence of the excess energy of the nonequilibrium electrons may be represented as a convolution of the pump pulse intensity envelope and the product of an exponential factor, with effective thermalization time  $\tau_{\text{th}}$ , and the Heaviside function

$$\Delta E(t) = \frac{A_0 \exp\left\{ \frac{\sigma^2}{16\tau_{\text{th}}^2 \ln 2} - \frac{t - t_0}{\tau_{\text{th}}} \right\}}{2} \times \left[ 1 + \operatorname{erf}\left( \frac{2\sqrt{\ln 2}(t - t_0)}{\sigma} - \frac{\sigma}{4\tau_{\text{th}}\sqrt{\ln 2}} \right) \right], \quad (3)$$

where  $A_0$  is the absorbed pump pulse energy per unit excited

volume,  $\sigma$  is the full width at half maximum of the pump pulse, and  $t_0$  is its time of arrival.<sup>26</sup> Since the measured film is thin compared to the ballistic electron range,<sup>15,16</sup> and because the pump spot size is much greater than the film thickness, the transient temperature gradients are small and so we can neglect heat transport. The modified two temperature model equations can then be written as

$$C_e \frac{\partial T_e}{\partial t} = -G(T_e - T_l) + \frac{\Delta E(t)}{\tau_{\text{th}}}, \quad (4)$$

$$C_l \frac{\partial T_l}{\partial t} = G(T_e - T_l), \quad (5)$$

where  $G$  is the electron-phonon coupling constant and  $C_l$  is the heat capacity of the lattice.

In the general case, these equations can be solved numerically. As shown in the Appendix, analytical solutions can be obtained in two limiting cases of high and low perturbation, and can then be joined together to describe the general case. The result is

$$t - t_0 = -\frac{A_e}{G}(T_e - T_{e,\text{max}}) - \frac{1}{\gamma} \ln \frac{T_e - T_{\text{equ}}}{T_{e,\text{max}} - T_{\text{equ}}}, \quad (6)$$

where  $T_{\text{equ}}$  and  $T_{e,\text{max}}$  are the final electron-lattice equilibration temperature and the maximum electron temperature, respectively.

This equation describes an initial linear decay of the transient temperature in the high perturbation limit,<sup>16</sup> and an exponential decay at longer time delays corresponding to the low perturbation limit. It may be used to fit the decay of the transient reflectivity signal once additional assumptions are made to relate the signal to the electron temperature.

## III. EXPERIMENT

Due to the finite absorption, the dielectric function of a metal is complex. In order to directly determine its real and imaginary parts, one can simultaneously measure the reflectivity and transmission of the sample,<sup>13-19</sup> if it is thin enough and deposited upon a transparent substrate. Since the real and imaginary parts of the dielectric function are related via Kramers-Kronig relations, each of them can be reconstructed from the other if the latter is measured over a sufficiently broad spectral range. The same is true regarding the transient reflectivity and transmissivity. Moreover, both are determined by the same single real function (the electron occupation number), or even by the same single real constant (electron temperature), if the electrons have thermalized. This means that in a time resolved experiment it is sufficient to measure either reflectivity or transmissivity, if the goal is to study electron dynamics rather than to check the Kramers-Kronig relations.

In our measurements we used the frequency doubled output of a Ti:Sapphire regenerative amplifier producing 200 fs pulses at a repetition rate of 1 kHz and wavelength of 800 nm. The beam was then split to generate pump and probe parts. The 400 nm pump pulse was generated through frequency doubling of the fundamental and had energy of

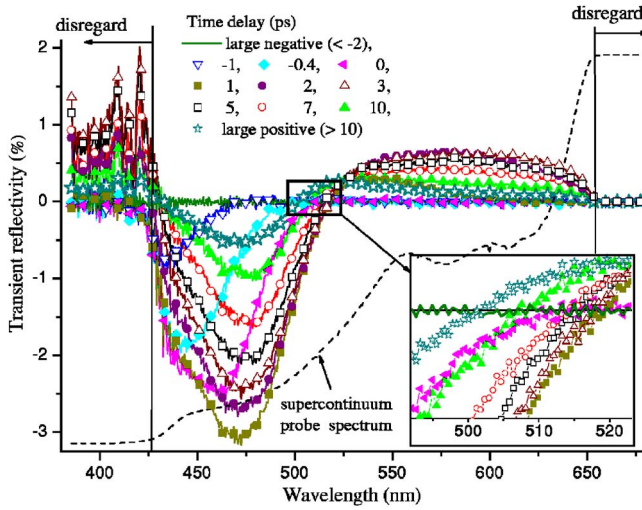


FIG. 1. (Color online) The transient reflectivity spectra are shown for different pump-probe time delays. The inset shows the shift of the zero crossing point with time delay. The white light continuum spectrum is shown by the dashed black line.

$2 \mu\text{J}$ . The other part of the fundamental was used to form a white light continuum (“supercontinuum”) in a 1 cm water cell. Both beams were p-polarized and focused onto the sample surface to give  $200 \mu\text{m}$  and  $400 \mu\text{m}$  diameter spots, for the probe and pump, respectively. The spots were carefully overlapped, while being viewed with a CCD camera. The angles of incidence of the pump and probe beams at the sample were  $35^\circ$  and  $30^\circ$ , respectively. The pump beam was passed through a delay line and reflected from an optogalvanic mirror just before the sample. The mirror was flipped between two positions so that every second pump pulse was deviated from the sample. The white probe beam was reflected from the sample and dispersed by a grating so that the different spectral components could be detected separately by a linear array detector. Signals with pump on and off were subtracted, normalized, and averaged over a time interval of 10 s. The water cell introduced a chirp within the probe pulse so that red light was delayed by about 2 ps with respect to the blue. Hence, we do not consider the delayed onset of reflectivity signals in different spectral regions but are concerned only with the intrinsic time scales for each component. The signal at different time delays was acquired in a random order to remove any slowly varying background.

#### IV. RESULTS AND DISCUSSION

The reflectivity spectra acquired at different time delays and the supercontinuum spectrum are shown in Fig. 1. For very short wavelengths (about 400 nm) the probe was too weak to produce meaningful results, while at very long wavelengths it was so strong that the detectors in the array were saturated. Hence, we will not consider the signal in these latter regions. At negative time delays, the signal vanishes over the entire spectral range as expected. At zero time delay, the signal appears first in the blue region and spans the entire range after approximately 2 ps. At later time delays,

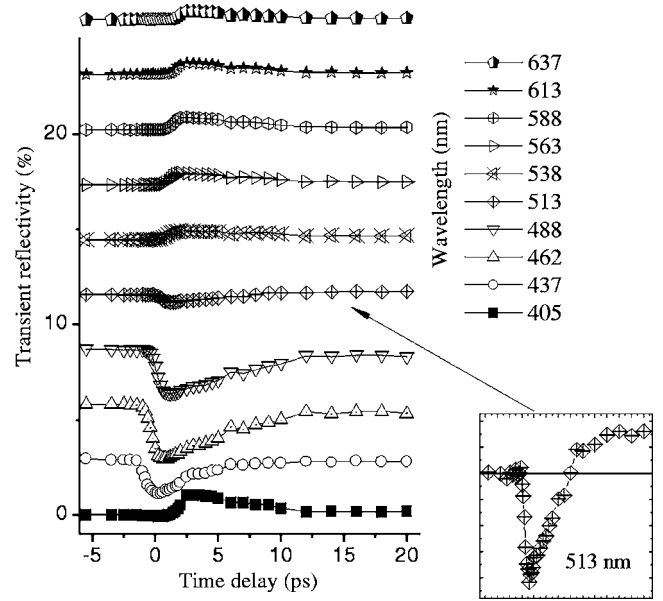


FIG. 2. The time resolved reflectivity signals constructed from the spectra in Fig. 1 are shown for different probe wavelengths.

the shape of the signal is bipolar with a zero crossing wavelength  $\lambda_x$  of about 510 nm.

Schoenlein *et al.* made a similar observation and interpreted it in terms of the transient temperature induced change of the Fermi-Dirac distribution (1), although with a temperature independent Fermi energy.<sup>12</sup> In their model, the zero crossing corresponds to the electron energy  $\varepsilon_x$  (relative to the top edge of the  $d$  band) at which the Fermi-Dirac distribution is unchanged by the optical excitation

$$f_{\text{FD}}(\varepsilon_x, T_0) = f_{\text{FD}}(\varepsilon_x, T_0 + \Delta T_e). \quad (7)$$

If the Fermi energy  $\varepsilon_F$  is constant, Eq. (7) can be satisfied only when  $\varepsilon_x$  is constant and equal to  $\varepsilon_F$ . However, our data show that the value of  $\lambda_x$  does not remain the same with changing time delay (and hence temperature), as shown in the inset of Fig. 1. As the electron temperature decreases at longer time delays, the value of  $\lambda_x$  decreases. Upon closer inspection, the same trend may be observed in the data of Schoenlein *et al.*<sup>12</sup> Surprisingly, if the temperature dependence of the Fermi energy (2) is taken into account, the zero crossing energy defined by Eq. (7) is

$$\varepsilon_x = \varepsilon_{F0} \left[ 1 + \frac{\pi^2 T_0 T_e}{12} \left( \frac{k_B}{\varepsilon_{F0}} \right)^2 \right], \quad (8)$$

and decreases as the electron temperature decreases. This shows that the transient reflectivity signal cannot be assumed proportional to the electron occupation number.

Let us now demonstrate that the assumption of proportionality between the transient reflectivity and the transient electron temperature is also inaccurate. By averaging the signal over wavelength ranges of a few tens of nanometers we were able to construct time resolved reflectivity signals for different wavelengths, which are shown in Fig. 2. While the shift in the onset of the signals is due to the chirp of the probe pulse introduced by the water cell, their temporal

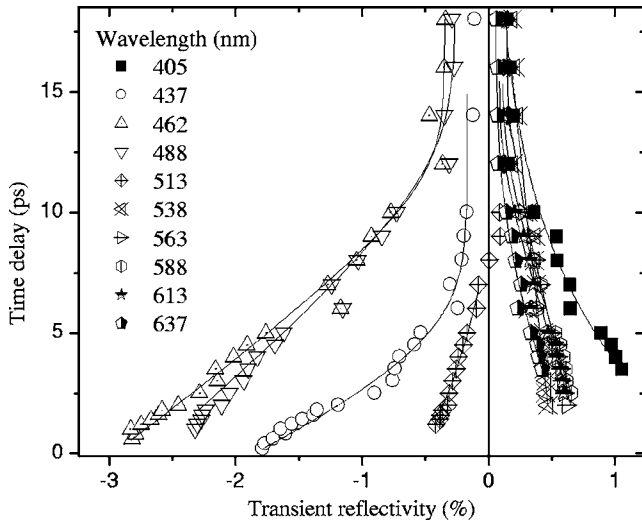


FIG. 3. The fit of the reflectivity signals shown in Fig. 2 is illustrated for various probe wavelengths. The symbols and solid lines represent the data points and the fitted curves, respectively.

shape also changes with the probe wavelength. In particular, the signal changes sign at a wavelength of 513 nm. The decaying part of the signals was fitted to Eq. (6), assuming first that the transient reflectivity is proportional to the electron temperature, and second a value of  $71 \frac{\text{J}}{\text{m}^3\text{K}^2}$  for the constant  $A_e$ .<sup>16</sup> The fitted curves are shown in Fig. 3. The fitting allowed us to extract values for the electron-phonon coupling constant and the electron-phonon equilibration temperature. The extracted electron-phonon coupling constant values are plotted against wavelength in Fig. 4. Although the error bars are in some cases quite large, the values are seen to depend upon the probe wavelength. Similarly strong wavelength dependence was observed in the values obtained for the electron-phonon equilibration temperature (not shown). At the same time, the electron-phonon coupling constant and the

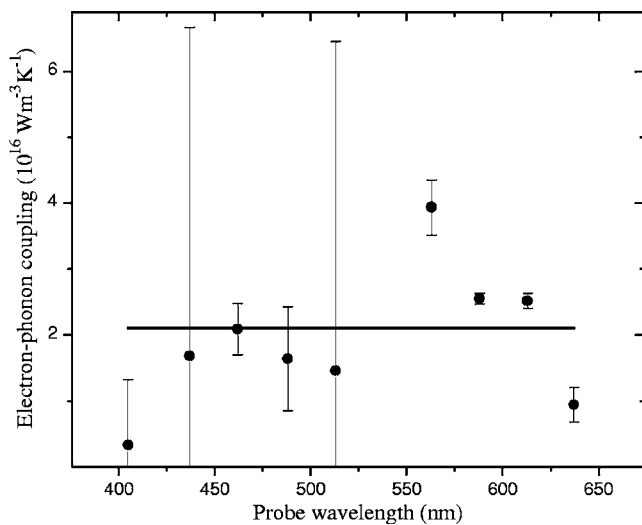


FIG. 4. The values of the electron-phonon coupling constant extracted from the fits shown in Fig. 3 are plotted against the probe wavelength. The solid line denotes the value of the constant derived in Ref. 16.

electron-phonon equilibration temperature are not expected to depend upon the wavelength. This shows that the transient reflectivity signal cannot be assumed to be proportional to the electron temperature, and that without a proper model for the reflectivity function of the sample, the relaxation times extracted from this kind of measurement cannot be reliably interpreted, particularly in the vicinity of the interband transition.

Let us consider more closely the bipolar signal observed at the probe wavelength of 513 nm. In Ref. 13, Sun *et al.* observed reflectivity signals from gold that changed sign in a way similar to that shown in Fig. 2. In their analysis, they assumed proportionality between the transient reflectivity on one hand, and the transient temperature and the number of nonthermalized electrons on the other. The sign change observed in their time resolved signals was then attributed to the competition between two contributions that are characterized by different relaxation times. Sun *et al.* did not measure the transient reflectivity spectra at different time delays, and hence did not observe the evolution of the zero crossing. However, they calculated the transient reflectivity spectra for different time delays, including the contribution from the nonthermalized electrons. Hohlfeld *et al.* calculated the spectra of the reflectivity change corresponding to various temperature changes, assuming that the electrons are completely thermalized.<sup>15,16</sup> The spectra calculated both by Sun *et al.* and by Hohlfeld *et al.* were similar to each other and to those measured in the present paper, and showed a similar shift of the zero crossing point. In light of this similarity, we suggest that nonthermalized electrons may not be responsible for the observation of bipolar time resolved signals, which originate instead from the inherent spectral dependence of the complex dielectric function and reflectivity. This conclusion is supported by our data showing that the shift of the zero crossing point persists at time delays longer than 10 ps, by which time the electron population has thermalized.

## V. SUMMARY

We have measured the transient reflectivity response of a thin film of gold. Using a supercontinuum pulse as a probe, we have been able to record transient reflectivity spectra over a wavelength range of about 300 nm for each value of the time delay. The wavelength at which the measured reflectivity changed sign has been found to depend upon the time delay, leading to bipolar time resolved signals. The wavelength dependence has been shown to contradict the simple model from Ref. 12, in which the signal was assumed to be proportional to the electron occupation number. At the same time, the spectra are qualitatively similar to those obtained from calculations that take into account the correct dependence of the reflectivity upon the dielectric function, and of the dielectric function upon the electron occupation number.<sup>13,15,16</sup>

Qualitatively, the shapes of the spectra do not seem to allow one to judge whether electrons are thermalized or not. Nevertheless, the quantitative analysis of our data has revealed that the shift of the zero crossing wavelength persists at time delays that are much longer than the time required for

electrons to thermalize. This suggests that the bipolar reflectivity signals do not necessarily imply a contribution from nonthermalized electrons, as has been assumed previously.

An analytical solution of the modified two temperature model equations has been used to extract the value of the electron-phonon coupling constant as function of the probe wavelength. The variation of the extracted values with wavelength confirmed that the interpretation of the transient reflectivity measurements may be unreliable unless a proper model for the dependence of the reflectivity upon the electron temperature is used.

#### ACKNOWLEDGMENTS

The authors acknowledge the financial support of the UK Engineering and Physical Sciences Research Council

(EPSRC) and the New Energy and Industrial Technology Development Organization (NEDO), M. Ali and B. J. Hickey for sample fabrication, A. T. G. Pym and B. K. Tanner for carrying out x-ray measurements, and the assistance of R. Wilks in setting up the apparatus.

#### APPENDIX

In the low perturbation limit when the excess electron temperature  $\Delta T_e$  is small compared to the ambient temperature, we neglect the dependence of the electronic heat capacity upon the electron temperature. The electronic heat capacity also depends upon the number of thermal electrons which can be assumed to be constant in this approximation. Then Eqs. (4) and (5) represent a system of coupled inhomogeneous linear differential equations of first order with constant coefficients. Such a system may be easily solved to give

$$\Delta T_e(t) = \frac{A_0}{2(C_l + C_e)} \left( \begin{array}{l} \left\{ 1 + \operatorname{erf}\left(\frac{2\sqrt{\ln 2}(t-t_0)}{\sigma}\right) \right\} \\ + q \left\{ 1 + \operatorname{erf}\left(\frac{2\sqrt{\ln 2}(t-t_0)}{\sigma} - \frac{\sigma\gamma}{4\sqrt{\ln 2}}\right) \right\} \exp(-\gamma(t-t_0)) \\ - s \left\{ 1 + \operatorname{erf}\left(\frac{2\sqrt{\ln 2}(t-t_0)}{\sigma} - \frac{\sigma}{4\tau_{\text{th}}\sqrt{\ln 2}}\right) \right\} \exp\left(-\frac{t-t_0}{\tau_{\text{th}}}\right) \end{array} \right), \quad (\text{A1})$$

where

$$q = \frac{C_l}{C_e(1 - \gamma\tau_{\text{th}})} \exp\left(\frac{\sigma^2\gamma^2}{16\ln 2}\right), \quad (\text{A2})$$

$$s = \left(1 + \frac{C_l}{C_e(1 - \gamma\tau_{\text{th}})}\right) \exp\left(\frac{\sigma^2}{16\tau_{\text{th}}^2\ln 2}\right), \quad (\text{A3})$$

and the electron-phonon relaxation rate is given by

$$\gamma = \frac{G(C_e + C_l)}{C_e C_l}. \quad (\text{A4})$$

In the high perturbation limit, one must take into account the linear dependence of the electronic heat capacity upon the transient temperature, i.e.,  $C_e = A_e T_e$ . Other simplifying assumptions must then be made in order to obtain an analytical solution. Let us assume that the lattice temperature remains constant during the experiment  $T_l = T_l^*$ , so that we need to consider only the transient electron temperature. This is justified because the heat capacity of the lattice is usually much greater than that of the electrons, and so the change in the temperature of the lattice is much smaller than that of the electrons. Let us also consider time scales longer than the electron-electron thermalization time but shorter than the characteristic time for heat transport. We may then rewrite Eq. (4) as

$$A_e T_e \frac{\partial T_e}{\partial t} = -G(T_e - T_l). \quad (\text{A5})$$

Applying the initial condition  $T_e(t_0) = T_{e,\text{max}}$ , integration yields

$$t - t_0 = -\frac{A_e}{G} \left( T_e - T_{e,\text{max}} + T_0 \ln \frac{T_e - T_0}{T_{e,\text{max}} - T_0} \right), \quad (\text{A6})$$

where the first term dominates at short time delays, for large perturbations when  $T_e \approx T_{e,\text{max}}$ , and the second term dominates at long time delays, for small perturbations when  $T_e \approx T_0$ .

Let us now analyze the behavior of solutions (A6) and (A1) for time delays sufficiently long that the difference between the transient electron and lattice temperatures is already very small, yet short enough that we can still neglect heat transport. For this time interval, we obtain from (A6)

$$T_e(t) \approx T_0 + \left[ (T_{e,\text{max}} - T_0) \times \exp\left(\frac{T_{e,\text{max}} - T_0}{T_0}\right) \right] \exp\left(-\frac{G}{A_e T_0}(t - t_0)\right), \quad (\text{A7})$$

and from (A1)

$$T_e(x,t) \approx T_{\text{equ}} + \frac{A_0 q}{C_l + C_e} \exp(-\gamma(t-t_0)), \quad (\text{A8})$$

where the final electron-lattice equilibration temperature is given by

$$T_{\text{equ}} = T_0 + \frac{A_0}{C_l + C_e}. \quad (\text{A9})$$

By comparing these two expressions, it is easy to construct a function that approaches (A6) at short time delays, where the excess electron temperature is very high and the temperature dependence of the electron heat capacitance cannot be neglected, but which also has the correct behavior, described by (A1), at longer time delays where the low perturbation solution is a good approximation. This may be done by substituting  $T_{\text{equ}}$  for  $T_0$ , and the relaxation rate  $\frac{G}{A_e T_0}$  for  $\gamma$  into (A6), resulting in Eq. (6) of the main text.

\*Email address: V.V.Kruglyak@exeter.ac.uk

<sup>1</sup>J. M. Kikkawa and D. D. Awschalom, Phys. Rev. Lett. **80**, 4313 (1998).

<sup>2</sup>E. Beaurepaire, J.-C. Merle, A. Daunois, and J.-Y. Bigot, Phys. Rev. Lett. **76**, 4250 (1996).

<sup>3</sup>T. Pfeifer, W. Kütt, H. Kurz, and R. Scholz, Phys. Rev. Lett. **69**, 3248 (1992).

<sup>4</sup>M. van Kampen, C. Jozsa, J. T. Kohlhepp, P. LeClair, L. Lagae, W. J. M. de Jonge, and B. Koopmans, Phys. Rev. Lett. **88**, 227201 (2002).

<sup>5</sup>S. V. Chekalin, V. M. Farztdinov, V. V. Golovlyov, V. S. Letokhov, Y. E. Lozovik, Y. A. Matveets, and A. G. Stepanov, Phys. Rev. Lett. **67**, 3860 (1991).

<sup>6</sup>S. D. Brorson, A. Kazeroonian, J. S. Moodera, D. W. Face, T. K. Cheng, E. P. Ippen, M. S. Dresselhaus, and G. Dresselhaus, Phys. Rev. Lett. **64**, 2172 (1990).

<sup>7</sup>V. V. Kruglyak, R. J. Hicken, M. Ali, B. J. Hickey, A. T. G. Pym, and B. K. Tanner, Phys. Rev. B **71**, 233104 (2005).

<sup>8</sup>V. V. Kruglyak, R. J. Hicken, M. Ali, B. J. Hickey, A. T. G. Pym, and B. K. Tanner, J. Opt. A, Pure Appl. Opt. **7**, S235 (2005).

<sup>9</sup>V. V. Kruglyak, A. Barman, R. J. Hicken, J. R. Childress, and J. A. Katine, Phys. Rev. B **71**, 220409(R) (2005).

<sup>10</sup>M. Mihailidi, Q. Xing, K. M. Yoo, and R. R. Alfano, Phys. Rev. B **49**, 3207 (1994).

<sup>11</sup>R. H. M. Groeneveld, R. Sprik, and A. Lagendijk, Phys. Rev. B **51**, 11433 (1995).

<sup>12</sup>R. W. Schoenlein, W. Z. Lin, J. G. Fujimoto, and G. L. Eesley, Phys. Rev. Lett. **58**, 1680 (1987).

<sup>13</sup>C.-K. Sun, F. Vallée, L. H. Acioli, E. P. Ippen, and J. G. Fujimoto, Phys. Rev. B **50**, 15337 (1994).

<sup>14</sup>N. Del Fatti, R. Bouffanais, F. Vallée, and C. Flytzanis, Phys. Rev. Lett. **81**, 922 (1998).

<sup>15</sup>J. Hohlfeld, U. Conrad, J. G. Müller, S. S. Wellershoff, and E. Matthias, in *Nonlinear Optics in Metals*, edited by K. H. Bennemann (Clarendon, Oxford, 1998).

<sup>16</sup>J. Hohlfeld, S. S. Wellershoff, J. Güdde, U. Conrad, V. Jähnke, and E. Matthias, Chem. Phys. **251**, 237 (2000).

<sup>17</sup>N. Del Fatti, C. Voisin, M. Achermann, S. Tzortzakos, D. Christofilos, and F. Vallée, Phys. Rev. B **61**, 16956 (2000).

<sup>18</sup>A. L. Dobryakov, S. A. Kovalenko, Y. E. Lozovik, S. P. Merkulova, V. M. Farztdinov, and N. P. Ernsting, JETP **92**, 267 (2001).

<sup>19</sup>R. Rosei and D. W. Lynch, Phys. Rev. B **5**, 3883 (1972).

<sup>20</sup>J. Y. Bigot, J.-C. Merle, O. Cregut, and A. Daunois, Phys. Rev. Lett. **75**, 4702 (1995).

<sup>21</sup>A. L. Dobryakov and Y. E. Lozovik, JETP Lett. **70**, 329 (1999).

<sup>22</sup>J. Y. Bigot, L. Guidoni, E. Beaurepaire, and P. N. Saeta, Phys. Rev. Lett. **93**, 077401 (2004).

<sup>23</sup>V. Halte, A. Benabbas, L. Guidoni, and J. Y. Bigot, Phys. Status Solidi B **242**, 1872 (2005).

<sup>24</sup>N. E. Christensen and B. O. Seraphin, Phys. Rev. B **4**, 3321 (1971).

<sup>25</sup>S. I. Anisimov, B. L. Kapeliovich, and T. L. Perelman, Zh. Eksp. Teor. Fiz. **66**, 776 (1974) [Sov. Phys. JETP **39**, 375 (1975)].

<sup>26</sup>V. V. Kruglyak and R. J. Hicken, J. Appl. Phys. **99**, 08P903 (2006).